Effects of Melt-to-Solid Volume Ratio and Pouring Temperature on Microstructures and Mechanical Properties of Cu/Al Bimetals in Compound Casting Process

CrossMark

GUOPING LIU, QUDONG WANG, LI ZHANG, BING YE, HAIYAN JIANG, and WENJIANG DING

Cu/Al bimetallic composites were fabricated by compound casting where aluminum melts were cast on Ni-coated Cu substrates. Effects of the melt-to-solid volume ratio (VR) and the pouring temperature on interfacial microstructures and mechanical properties of Cu/Al bimetals were investigated systematically. Results show that a continuous and compact interface can be formed when the pouring temperature exceeds 953 K (680 °C). When the VR or pouring temperature increases, the solidification time of α(Al) increases, resulting in an increase in the dissolution content of Cu substrate. The transition zone consists of α(Al) + Al_2Cu eutectic layer and intermetallic compounds (IMCs) layer, and the IMCs are identified as Al_2Cu, $AlCu$, and Al_4Cu_9. Ni coating participates in the formation of AlCuNi phase between the Al_2Cu layer and AlCu layer when the pouring temperature is 973 K (700 °C). The presence/absence of Ni-containing phase has a close relationship with the dissolution of the Cu substrate. Shear-strength tests show that shear fracture mainly occurs at the hard brittle IMCs layer, and the highest shear strength of 36.01 MPa is obtained for the samples fabricated at 993 K + VR 49.24 (720 °C + VR 49.24).

I. INTRODUCTION

BIMETALLIC composites are commonly used in various industrial fields, such as heat-transfer, electrical, and transportation industries.[1] Numerous bimetals have been fabricated, e.g., Al/Al,[1,2] Mg/Al,[3,4] Fe/Al,[5] Ti/Al,[6] and Cu/Al.[7] Among these bimetals, Cu/Al bimetal, which combines the good electrical and thermal conductivities of Cu with the low density and corrosion resistance of Al, has attracted great attention across the whole world.[8–10] Although compound casting method has exhibited great superiority in fabricating irregular shapes of Cu/Al bimetallic composites,[11] it still has some drawbacks in the aspects of the rapid growth of IMCs and the oxidation of the solid Cu substrate.[12]

It is confirmed that five IMCs (i.e., Al_2Cu, $AlCu$, Al_3Cu_4, Al_2Cu_3, and Al_4Cu_9) are prone to be formed at the interface.[13,14] IMCs of a certain thickness can improve the interfacial bonding strength. However, Lee et al. claimed that a thicker IMCs layer could seriously degrade the tensile strength of Cu/Al metal joints.[15] It has been reported that the critical thickness of IMCs is about 2.5 μm for Cu/Al bimetals produced by cold roll welding method.[16] When the thickness of the IMCs layer exceeds that of a critical value, the interfacial bond strength will deteriorate greatly. Su et al.[17] found that when the thickness of the IMCs layer increases from 1.2 to 33.7 μm, the interfacial shear strength decreases from 67.9 to 40.5 MPa for the Cu/Al bimetals produced by core-filling continuous casting process. Therefore, the study of methods to control the growth of Cu-Al IMCs is of great significance.

On the other hand, Cu bar is easy to be oxidized at elevated temperatures, and the grown oxide film would inhibit the solid–liquid bonding.[18] To tackle this problem, researchers have laid great attention focusing on planting thin coating layers on the Cu substrate before the solid–liquid bonding process, such as Zn layer,[18] Ni-P layer,[12] and Ni layer.[19] As described above, redundant IMCs at the interface would greatly weaken the mechanical and electrical properties of Cu/

GUOPING LIU, QUDONG WANG, LI ZHANG, BING YE, HAIYAN JIANG, and WENJIANG DING are with the National Engineering Research Center of Light Alloy Net Forming and State Key Laboratory of Metal Matrix Composites, School of Materials Science and Engineering, Shanghai Jiao Tong University, 200240, Shanghai, P.R. China. Contact e-mail: wangqudong@sjtu.edu.cn

Al bimetals. It is an urgent need to find a coating material that can protect the substrate and inhibit the rapid growth of IMCs. Ni coating is a good candidate, and it has shown good effects in Mg/Al and Fe/Al bimetals. Han used the Ni layer to modify the intermetallic phases which were formed during a chemical reaction between the molten aluminum and the steel insert.[20] Sun et al.[21] and Wang et al.[22] found that the Ni interlayer can effectively restrain the formation of Mg-Al intermetallics during the hybrid welding of Mg to Al.

According to the phase diagrams of Al-Ni[23] and Cu-Ni,[24] Ni has maximum solid solubilities of 6.1 (wt pct) and 100 (wt pct) in Al and Cu matrixes, respectively, and it could be a suitable coating material for the casting-bonded Cu/Al bimetals. It has been found that the Ni interlayer can effectively restrain formation of Cu-Al IMCs based on the research of Zhao et al.[19] Hu et al.[12] deposited an Ni-P coating on the Cu substrate, and they identified that the Ni-P interlayer can effectively inhibit the formation of Cu-Al IMCs by acting as a diffusion barrier and protective film. However, few studies have been conducted on the reaction mechanism between Ni layer and adjacent substrates in Cu/Al bimetals.

Although Ni coating has been applied to inhibit the formation of IMCs in Cu/Al bimetals, how the Ni coating participates in the formation of IMCs for Cu/Al bimetals fabricated at different processing parameters during compound casting still needs further study. This study investigates the interfacial microstructural evolution and mechanical properties of Ni-coated Cu/Al bimetals at different melt-to-solid volume ratios (VRs) and pouring temperatures. Interfacial temperature–time curves were monitored by a real time computer-aided recording system. The interfacial bonding strength and Vickers microhardness of Cu/Al bimetals were evaluated simultaneously. The underlying reaction mechanisms between the Ni coatings and adjacent substrates, and the interfacial fracture mechanisms are studied in detail.

II. MATERIALS AND METHODS

Commercial T2 Cu bars with the dimensions of $5 \times 5 \times 50$ mm^3 and $12 \times 12 \times 50$ mm^3 were used as the solid insert materials. Pure Al casting ingots with 99.7 pct purity were prepared for the casting materials. Cu bars were first treated with brush scratching, degreasing, alkali cleaning, and 30 pct nitric acid pickling in sequence, and then a Ni layer was coated on the Cu bars according to the electroplating process reported in the literature.[25] The Ni-plating electrolytes included 350 g nickel sulphate (Ni_2SO_4), 50 g nickel chloride ($NiCl_2 \cdot 6H_2O$), and 1 L deionized water. The operating plating voltage was 8 volts and the plating time duration was 12 minutes. The thickness of Ni coating is about 4 μm, as presented in Figure 1.
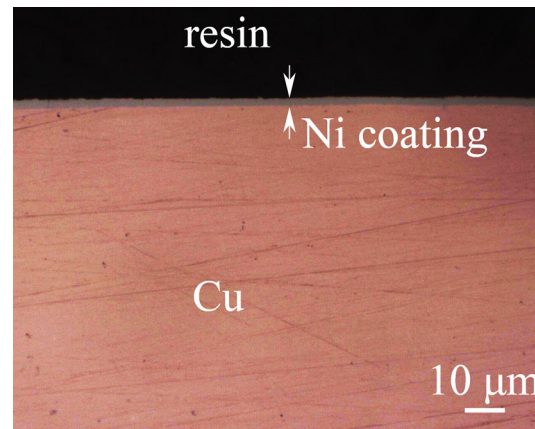

Fig. 1—Optical image of the cross section of a Cu bar with Ni coating.

$12 \times 12 \times 50$ mm^3 and $5 \times 5 \times 50$ mm^3 Ni-plated Cu bars were mounted on the left and right cavities of the mold, respectively, as illustrated in Figure 2(a). Then the mold and Cu bars were preheated at 373 K (100 °C) for 30 minutes. The Al ingots were melted in an electric resistance furnace. After degasing and refining, the Al melts were poured into the mold at the temperatures of 953 K, 973 K, and 993 K (680 °C, 700 °C, and 720 °C), respectively. K-type thermocouples were welded on the surface of the Cu bars to record the temperature of Al near the interface during compound casting. A heat-resisting material which was made of alkali-free glass fiber was sheathed on the thermocouple to ensure a good contact, and it was a hollow tube with a diameter of 3 mm. The temperature–time curves were monitored by a real time computer-aided recording system. The obtained Cu/Al bimetals are displayed in Figures 2(b) and (c). The VR in the present study can be calculated by the equation[4]:

$$\text{VR} = \frac{V_a}{V_m} = \frac{\pi r^2 h - a^2 h}{a^2 h} = \pi \left(\frac{r}{a}\right)^2 - 1, \qquad [1]$$

where V_a and V_m are the effective volumes of the Al melt and mold, respectively, r is the radius of the cavity, and a is the length of the Cu bars, h is the height of the Cu bar. The VRs are calculated as 7.72 and 49.24 for the $12 \times 12 \times 50$ mm^3 and $5 \times 5 \times 50$ mm^3 Ni-plated Cu bars, respectively.

An electrodischarge cutting machine was used to cut Cu/Al bimetallic disks for microstructural analysis and mechanical properties evaluation. As shown in Figure 2(b), Cu/Al bimetallic disks were cut with a same thickness of 7 mm. The third disk (③) was used for metallographic observation, and the other samples were used for mechanical properties evaluation. Interfacial microstructures were observed by a LEICA MEF4M optical microscopy (OM). IMCs were analyzed on a NOVA Nano 230 scanning electron microscopy (SEM) equipped with X-ray energy dispersive spectroscopy
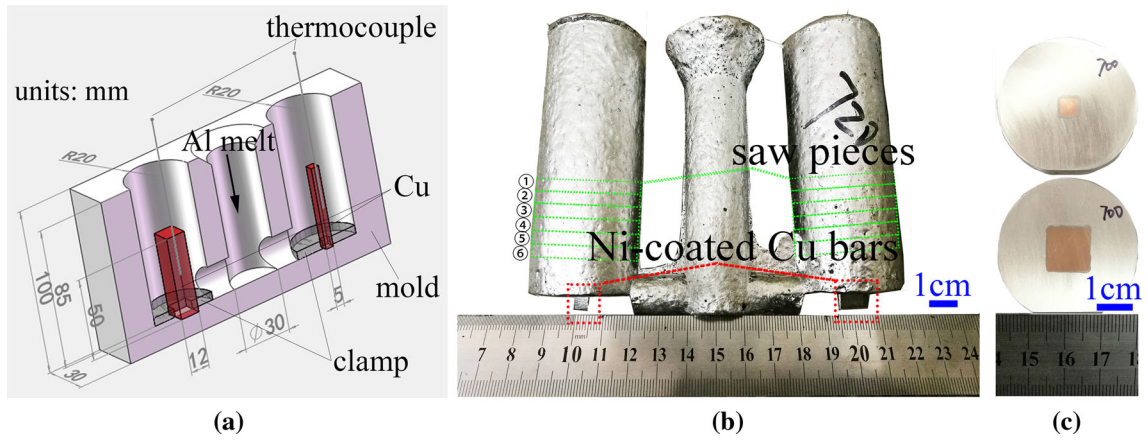
Fig. 2—Schematic illustration of the compound casting process (*a*), the as-received Cu/Al bimetals (*b*), and the Cu/Al bimetallic disks (*c*).
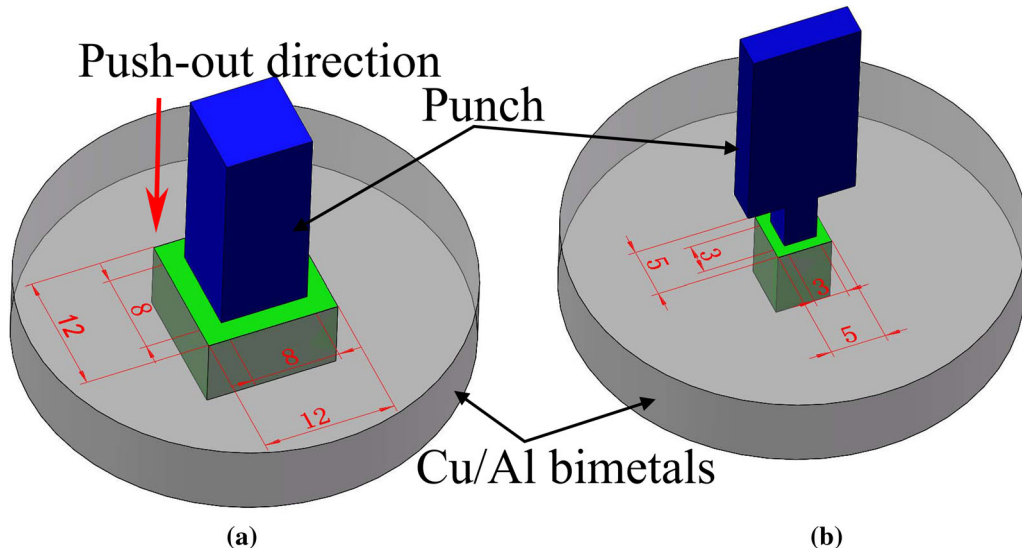

Fig. 3—Schematic illustration of the push-out test for different Cu/Al bimetallic samples (units: mm): (*a*) VR 7.72; (*b*) VR 49.24.

(EDS). X-ray diffraction (XRD) and electron backscatter diffraction (EBSD) were used to detect the IMCs at the interface. Image Pro Plus 6.0 software was used to measure the average thicknesses of the IMCs. Push-out test was applied to assess the interfacial shear strength. Figure 3 shows the schematic illustration of the push-out test for Cu/Al bimetals at ambient temperature. A high-strength steel was machined to two different punches. The dimentions of the contact surface between the punch and Cu/Al bimetals with VR 7.72 and VR 49.24 are 8×8 mm^2 and 3×3 mm^2, respectively. The upper side of each punch was fixed on a Zwick/Roell-20 kN test machine; the lower side of each punch was pushed to contact with the copper substrate. The indenter moving rate for the push-out test is 0.5 mm/min. The shear strength (τ) is calculated by $\tau = F/4Lh$, where F is the maximum load, L is the width of the Cu bars, and h is the specimen disk thickness. At least three specimens were measured under each condition. Micro Vichers hardness across the interface was measured on a

Zwick/Roell/zhμ machine at a load of 25 g and a dwell time of 15 second.

III. RESULTS

A. Cooling Curves

Figure 4 shows the cooling curves of Cu/Al bimetals at different VRs and pouring temperatures. When the Al melts come to contact with the Cu bars, an instant temperature increase occurs. Then the cooling curve profiles vary in two different ways for the VR 7.72 bimetallic samples: a slow temperature increase in the form of a smooth arc for the samples pouring at 953 K and 973 K (680 °C and 700 °C); a quick descent from the highest temperature, staying at roughly 933 K (660 °C) about 8 seconds for the sample pouring at 993 K (720 °C), as is seen from the local magnification zone in Figure 4(a). The plateau is deemed to be the
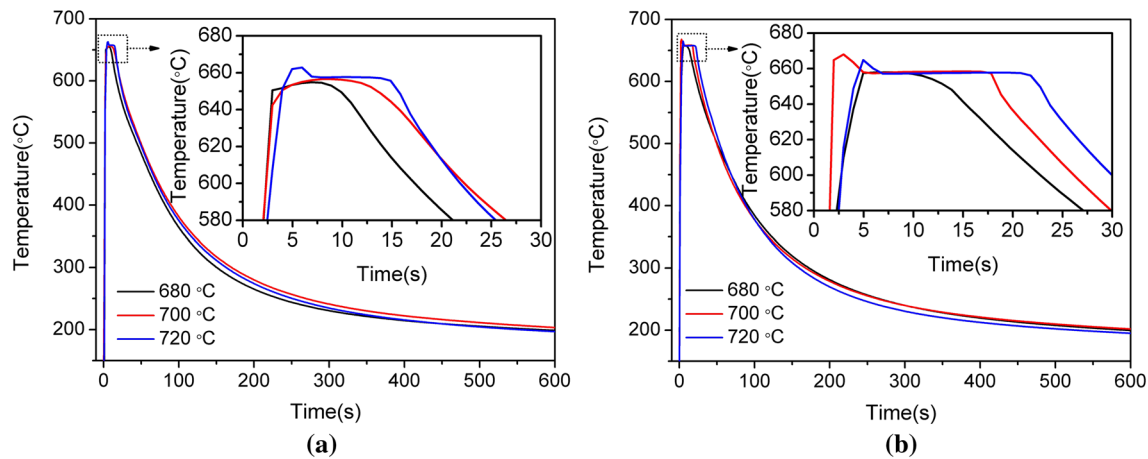
Fig. 4—Cooling curves of Cu/Al bimetals produced at different VRs: (*a*) VR 7.72; (*b*) VR 49.24.

solidification of α(Al), as reported by Pintore et al.[26] Cooling curves for the VR 49.24 samples at different pouring temperatures shown in Figure 4(b) display the similar profiles as the 993 K + VR 7.72 (720 °C + VR 7.72) Cu/Al bimetals. The main differences are the solidification times of α(Al). The solidification time of α(Al) increases when the pouring temperature increases from 953 K to 993 K (680 °C to 720 °C). In order to further study the interfacial phase transformation, the first-derivative curves are obtained.

Figure 5 shows the cooling curves and the corresponding first-derivative curves of Cu/Al bimetals fabricated at different VRs and pouring temperatures. Some characteristic points on the cooling curves can be clearly seen. Based on dT/dt = 0, the solidification time of α(Al) (t_0) can be calculated. For the samples of 973 K + VR 49.24, 993 K + VR 7.72 and 993 K + VR 49.24 (700 °C + VR 49.24, 720 °C + VR 7.72 and 720 °C + VR 49.24), the corresponding solidification times (t_0) are recorded as 11, 5 and 12 seconds, respectively. The α(Al) solidification time has a close relationship with the dissolution of solid Cu substrates, and it will be discussed in the Section IV–A. As solidification continues, a new phase nucleates at about 897 K (624 °C) with a sudden change in derivative, as indicated in position *A* in Figures 5(b) and (d). According to the research of Pintore et al.[26] it means the formation of Al$_2$Cu phase. The eutectic reaction is captured at position *B* with the formation temperature of 821 K (548 °C) for relatively high pouring temperature Cu/Al bimetals. The average cooling rate (CR) was calculated by the equation:[27,28] CR = $(T_1 - T_s)/(t_s - t_1)$, where T_1 and T_s are the liquidus and solidus temperatures, respectively; t_1 and t_s are the times from the cooling curve corresponding to the liquidus and solidus temperatures, respectively. The cooling rates for Cu/Al bimetals fabricated at 973 K + VR 7.72, 993 K + VR 7.72, 973 K + VR 49.24, and 993 K + VR 49.24 (700 °C + VR 7.72, 720 °C + VR 7.72, 700 °C + VR 49.24, and 720 °C + VR 49.24) are 4.01, 4.18, 3.54, and 3.22 K/s, respectively. When the VR increases from 7.72 to 49.24,

the cooling rate always decreases for the Cu/Al samples produced at 973 K and 993 K (700 °C and 720 °C).

B. Microstructure

Figure 6 shows the typical interfacial microstructures of Cu/Al bimetals at different VRs and pouring temperatures. When the pouring temperature is 953 K (680 °C), the Cu substrates will obtain less energy from the Al melt to activate the interface reaction, so there is no obvious transition layer on the interface. However, when the pouring temperature increases to 973 K and 993 K (700 °C and 720 °C), a relatively uniform interface is formed, and the thickness of the transition zone for Cu/Al bimetals fabricated at VR 7.72 increases to 617 and 1138 μm, respectively; the thickness of the transition zone for Cu/Al bimetals fabricated at VR 49.24 increases to 859 and 1152 μm, respectively. The interfaces between the transition zones and Cu substrates are all displayed in a wave-like shape, indicating the non-uniform dissolution of the Cu substrates under different process conditions. Figures 7(a) through (d) present the SEM image of Cu/Al bimetal produced at 953 K + VR 7.72 (680 °C + VR 7.72) and the corresponding concentration mappings of Al, Ni, and Cu. As shown in Figure 7(a), some gaps exist at the interface. A continuous thin Ni layer exists at the interfacial region, indicating that the Ni coating has not been absolutely dissolved into the molten Al at relatively low pouring temperature and VR. It is also found that few Al atoms have diffused into the Cu substrates (Figure 7(b)), while the Ni atoms have diffused into both the adjacent Cu and Al substrates (Figure 7(c)), and the Cu atoms have diffused into the Al substrate through the Ni interlayer (Figure 7(d)). Figure 7(e) shows the magnified interfacial microstructure of 953 K + VR 49.24 (680 °C + VR 49.24) Cu/Al bimetal. Flake-like Al$_2$Cu phase is observed near the interface at the Al substrate, which shows a good accordance with the cooling curve shown in Figure 5(b). Some gaps are clearly seen at the interface, which indicates that the molten Al does not
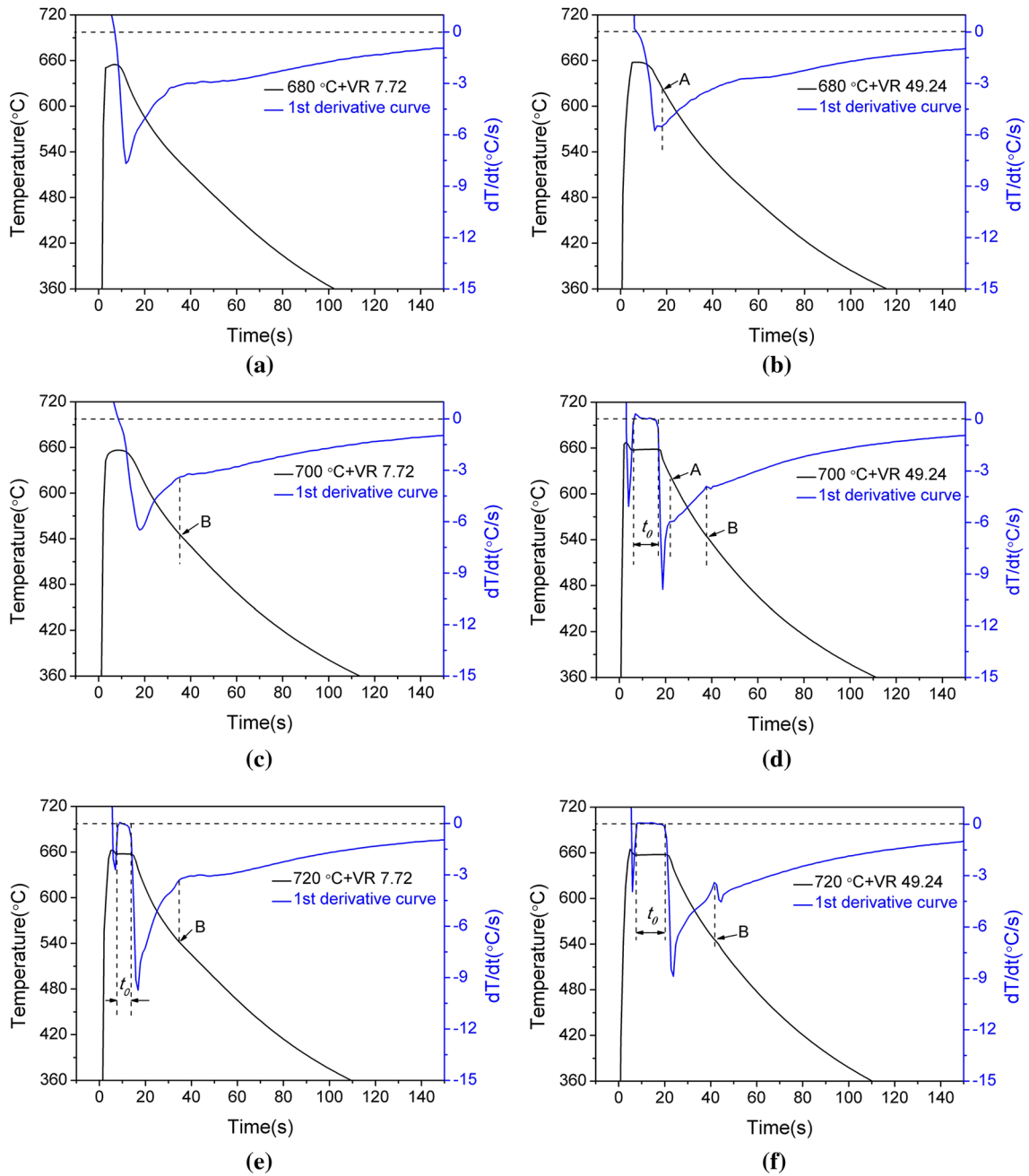
Fig. 5—Cooling curves and first-derivative curves of the Cu/Al bimetals produced at different processing parameters: (*a*) 680 °C + VR 7.72; (*b*) 680 °C + VR 49.24; (*c*) 700 °C + VR 7.72; (*d*) 700 °C + VR 49.24; (*e*) 720 °C + VR 7.72; (*f*) 720 °C + VR 49.24. Position *A* corresponds to the nucleation of Al₂Cu, and position *B* corresponds to the eutectic reaction.

melt the Ni coating completely and a metallurgical bonding fails to form between the Cu layer and Al layer at 953 K (680 °C). It should be noted that there may be formed Al-Ni and Cu-Ni intermetallic compounds[29] at the interface for the Cu/Al bimetals fabricated at 953 K (680 °C). Therefore, Cu/Al bimetals pouring at 973 K and 993 K (700 °C and 720 °C) with continuous interfaces are the main research subjects in the following part. On the other hand, the thicknesses of the dissolved Cu substrate (d_{Cu}) are measured, and the results are shown in Table I. It is found that the Cu/Al bimetals

produced at high VRs and pouring temperatures have larger d_{Cu} values.

To further investigate the microstructural evolution of Cu/Al bimetals produced at different processing conditions, the metallographic microstructures with higher magnification are obtained from three typical positions of the transition zone, *i.e.*, the near-aluminum region, the middle region of the transition zone, and the near-copper region, as presented in Figure 8. The transition zone can be divided into two layers: layer I is mainly composed of IMCs, and layer II is primarily
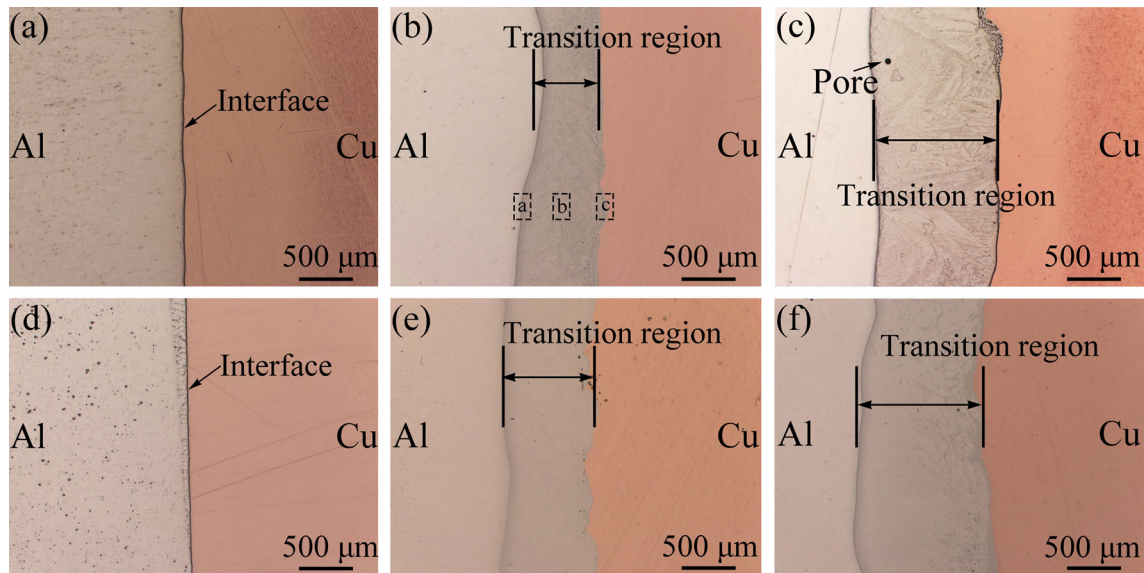
Fig. 6—OM images of the Cu/Al bimetals produced at different processing parameters: (*a*) 680 °C + VR 7.72; (*b*) 700 °C + VR 7.72; (*c*) 720 °C + VR 7.72; (*d*) 680 °C + VR 49.24; (*e*) 700 °C + VR 49.24; (*f*) 720 °C + VR 49.24.
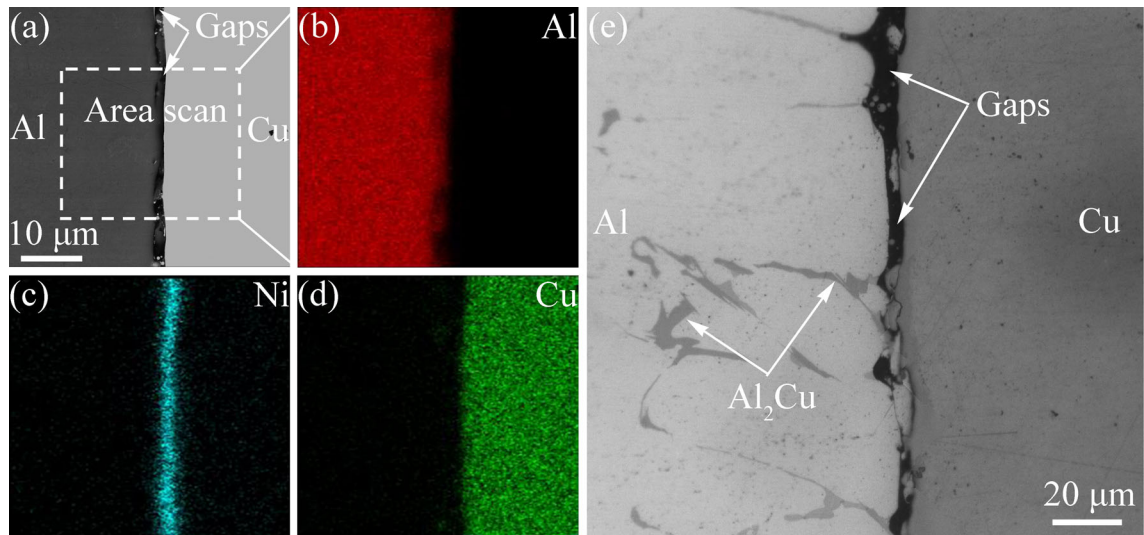

Fig. 7—SEM image of 680 °C + VR 7.72 Cu/Al bimetal (*a*) and its local chemical elements mappings of Al, Ni, and Cu shown in (*b* through *d*), respectively; magnified OM image showing the interfacial microstructure of 680 °C + VR 49.24 Cu/Al bimetal (*e*).

the α(Al) + Al$_2$Cu eutectics. It is interesting to find that the types and morphologies of IMCs vary with the increasing pouring temperatures. Some dispersed phases grow on the Cu-rich intermetallics and stretch into the bulk Al$_2$Cu for the Cu/Al samples at 973 K (700 °C). However, when the pouring temperature increases to 993 K (720 °C), these phases disappear. The presence/absence of the new phases is closely related to the Ni coating and pouring temperatures, and it will be discussed in the Section IV–A. Some bulk Al$_2$Cu phase grows adjacent to the IMCs layer. Layer I seems to have a larger thickness for Cu/Al bimetals pouring at 973 K (700 °C) than that pouring at 993 K (720 °C). At the middle region of the transition zone, the eutectics occupy the main microstructure, and some dispersed

Al$_2$Cu phases are also detected. The α(Al) + Al$_2$Cu eutectics are observed in lamella and anomalous morphologies. The anomalous eutectics seem like networks growing across the transition zone, which are surrounded by the lamella eutectics.

Figures 9(a) through (d) display SEM images of the Cu/Al bimetals produced at different VRs and pouring temperatures. Four kinds of IMCs are formed on the layer I with different morphologies and contrasts at 973 K (700 °C). However, when the pouring temperature increases to 993 K (720 °C), the dispersed phase which grows in a perpendicular orientation to the interface disappears. The IMCs were detected by EDS, and the corresponding results are presented in Table II. The IMCs are identified as Al$_4$Cu$_9$, AlCu, and Al$_2$Cu in

Table I.   Thicknesses of the Dissolved Cu Substrate (d_{Cu}) at Different Processing Parameters

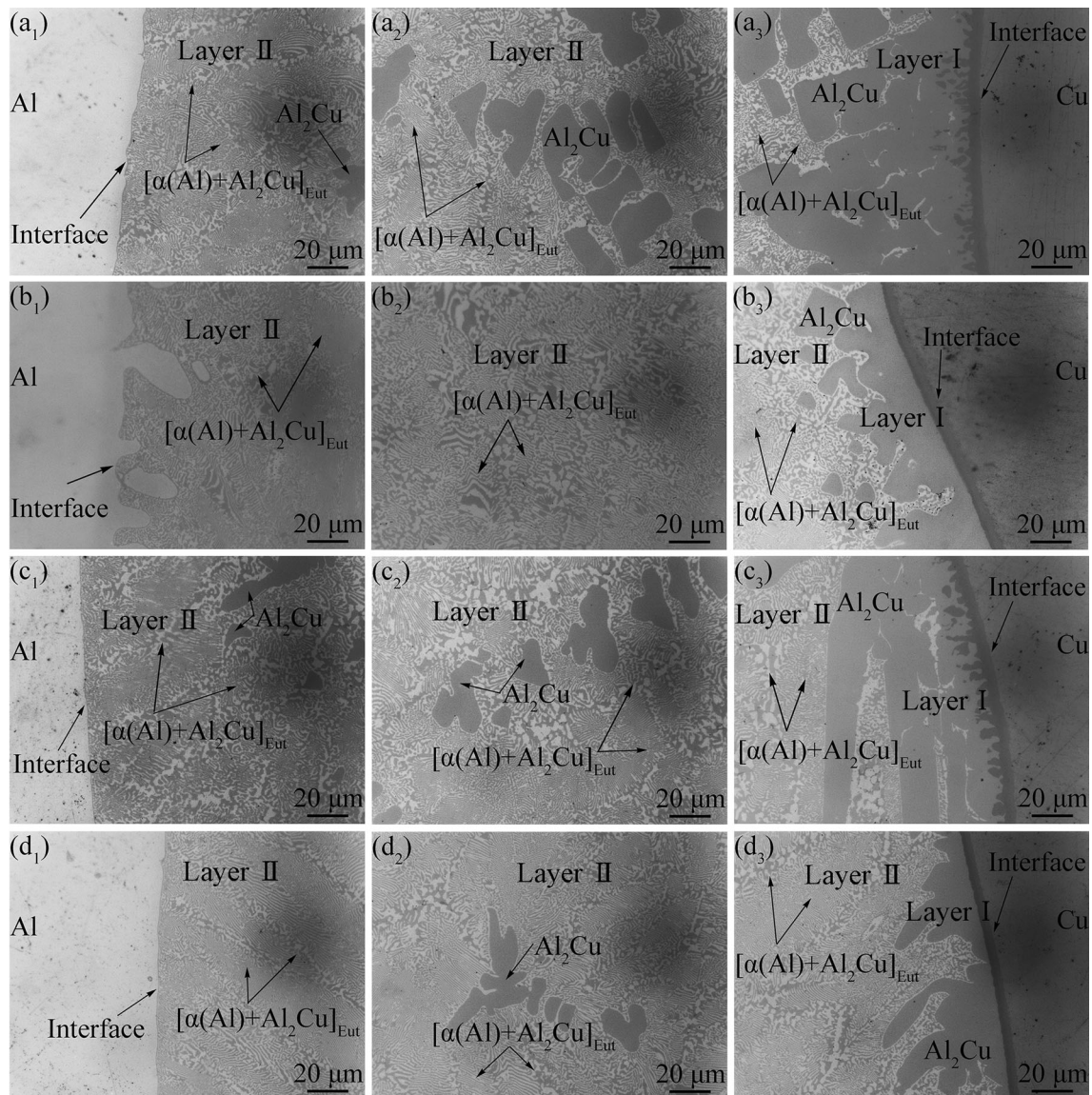| Cu/Al	700 °C + VR 7.72	720 °C + VR 7.72	700 °C + VR 49.24	720 °C + VR 49.24
d_{Cu} (μm)	79.3 ± 8.1	191.3 ± 4.6	112 ± 8.2	226 ± 6.6

Fig. 8—The typical interfacial microstructures in three characteristic regions identified in Fig. 5(b). (a_1 through d_1) correspond to the near-aluminum region under the conditions of 700 °C + VR 7.72, 700 °C + VR 49.24, 720 °C + VR 7.72, and 720 °C + VR 49.24, respectively; (a_2 through d_2) correspond to the middle region of the transition zone under the conditions of 700 °C + VR 7.72, 700 °C + VR 49.24, 720 °C + VR 7.72, and 720 °C + VR 49.24, respectively. (a_3 through d_3) correspond to the near-copper region under the conditions of 700 °C + VR 7.72, 700 °C + VR 49.24, 720 °C + VR 7.72, and 720 °C + VR 49.24, respectively.

sequence from the Cu layer to the eutectic layer. Ni atoms participate in the formation of an AlCuNi phase between the Al_2Cu layer and the AlCu layer with the Ni concentration of 1 ~ 2 (wt pct) at 973 K (700 °C). The AlCuNi phase needs to be further characterized in the future research. Figure 9(e) shows the EBSD analysis of IMCs distribution on the Cu/Al bimetal produced at 993 K + VR 7.72 (720 °C + VR 7.72). The IMCs are identified as Al_4Cu_9, AlCu, and Al_2Cu. These results are well in agreement with EDS results. Figure 10 presents the EDS line scanning analysis of the IMCs layer along the marked-up lines in Figure 9. The relative contents of Cu and Al atoms across the Al_2Cu phase remain almost constant. However, there exist Al(Cu) concentration gradients for the AlCu, AlCuNi, and Al_4Cu_9 phases. It is also confirmed from Figure 10 that Ni atoms only
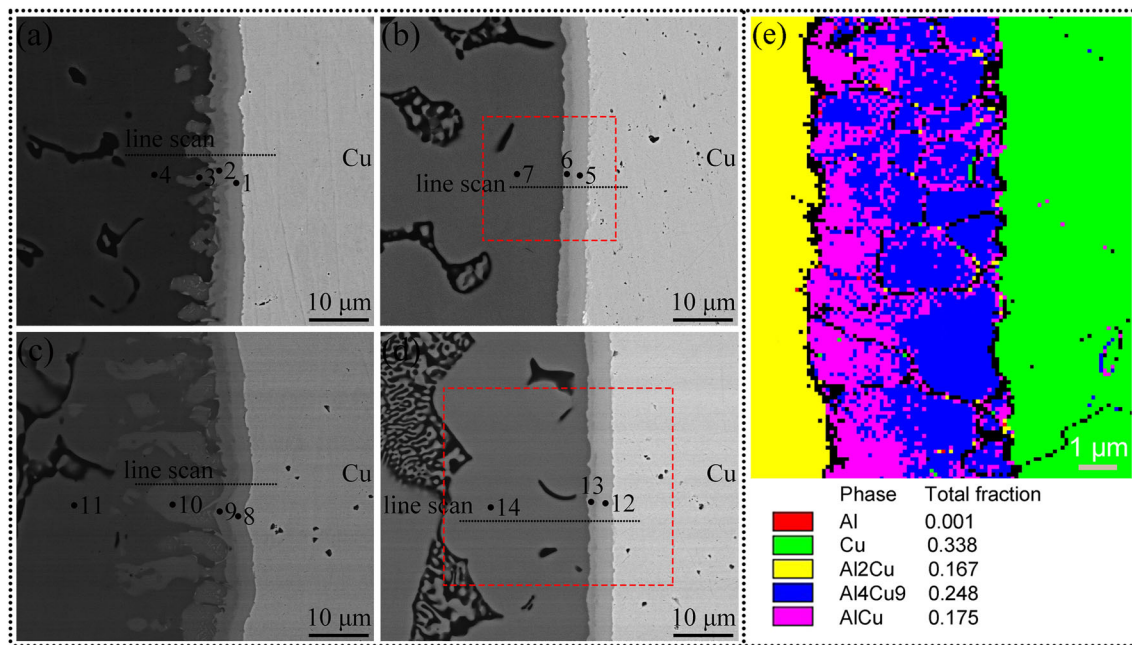
Fig. 9—SEM images of Cu/Al bimetals produced at different processing parameters: (*a*) 700 °C + VR 7.72; (*b*) 720 °C + VR 7.72; (*c*) 700 °C + VR 49.24; (*d*) 720 °C + VR 49.24; (*e*) EBSD phase image identifying the IMCs layer for Cu/Al bimetal fabricated at 720 °C + VR 7.72.

exist on the AlCuNi phase, and the other IMCs or Cu matrix has excessively low content of Ni. In order to evaluate the presence and distribution of Ni for the Cu/Al bimetals fabricated at 993 K (720 °C), concentration mappings of Al, Ni, and Cu near the interfacial region (see the red dash lines in Figures 9(b) and (d)) are shown in Figure 11. It is found that the Ni atoms are uniformly distributed in both the Cu substrate and adjacent IMCs for Cu/Al bimetals produced at different VRs.

In the current study, since the average thickness of Al_2Cu exceeds 15 μm, which is far higher than the other IMCs, only the thicknesses of Al_4Cu_9, AlCu, and Al_4Cu_9 + AlCu are calculated, and the results are presented in Figure 12. The thickness of AlCu phase decreases obviously with the increasing pouring temperature, while the thickness of Al_4Cu_9 phase remains almost constant. The presence of the AlCuNi phase is responsible for this change. For the Cu/Al bimetals pouring at 993 K (720 °C), when the VR increases from 7.72 to 49.24, the thickness of AlCu phase decreases from 1.5 to 1.1 μm, while the thickness of Al_4Cu_9 phase remains almost constant.

C. *Interfacial Shear Strength*

Figure 13 shows the interfacial shear strength of Cu/Al bimetals produced under different processing conditions. The Cu/Al bimetallic samples pouring at 993 K (720 °C) have a higher shear strength than those pouring at 973 K (700 °C), and the Cu/Al bimetals produced at 993 K + VR 49.24 (720 °C + VR 49.24) have the highest shear strength of 36.01 MPa. The interfacial shear strength seems to have an inversely proportional relationship with the thickness of AlCu in

the present study. Cross-sectional images and typical fractographs of the shear fractured Cu/Al bimetals are presented in Figure 14, and the phases indicated by arrows are identified by EDS. As shown in Figures 14(a$_1$) through (d$_1$), some IMCs remain on the shear fractured Cu substrates. In the Cu/Al sample produced at 720 °C + VR 49.24, a crack was found through the eutectic structure. Some fractured bulk Al_2Cu phases are observed on both the Al side and Cu side. The AlCu phase displays the convex shape on the fractured Al side and coupled concave shape on the fractured Cu side. When the cross-sectional images are combined with the corresponding fractographs, it was found that interfacial fracture mainly occurred at the IMCs layer. Trace AlCuNi and Al_4Cu_9 phases are detected on the Al side, as shown in Figures 14(b$_2$) and (c$_2$). Figure 15 shows XRD patterns on the fractured Cu/Al bimetals fabricated at 973/993 K + VR 7.72 (700/720 °C + VR 7.72). Al_2Cu and AlCu are identified on the Al side. All the three IMCs (Al_2Cu, AlCu, and Al_4Cu_9) are identified on the Cu side. However, Ni-containing phase is not found in the Cu/Al bimetal fabricated at 973 K + VR 7.72 (700 °C + VR 7.72). These results are consistent with SEM analysis.

D. *Microhardness*

Figure 16 shows the microhardness indentations and microhardness profiles across the transition zone of Cu/Al bimetals produced at different VRs and pouring temperatures. It is found that the Al_2Cu phase (see the red dashed circles in Figure 16(a)) has higher hardness values than both the adjacent substrates and eutectics regions. It is the IMCs layer that makes the

Table II. EDS Results of Cu/Al Bimetals Produced at Different Processing Parameters Shown in Fig. 9

	700 °C + VR 7.72				720 °C + VR 7.72				700 °C + VR 49.24			720 °C + VR 49.24		
	1	2	3	4	5	6	7	8	9	10	11	12	13	14
Cu (Wt Pct)	78.9	69.2	58.2	52.7	77.6	68.4	52.8	79.4	70.5	60.9	52.5	78.7	68.9	52.4
Al (Wt Pct)	21.1	30.8	40.1	47.3	22.4	31.6	47.2	20.6	29.5	38.0	47.5	21.3	31.3	47.6
Ni (Wt Pct)	0	0	1.7	0	0	0	0	0	0	1.1	0	0	0	0
Possible phase	Al$_4$Cu$_9$	AlCu	AlCuNi	Al$_2$Cu	Al$_4$Cu$_9$	AlCu	Al$_2$Cu	Al$_4$Cu$_9$	AlCu	AlCuNi	Al$_2$Cu	Al$_4$Cu$_9$	AlCu	Al$_2$Cu

microhardness increase sharply. When combining the microhardness profiles with the as-received microstructures, it is easy to find that the microhardness of Al-Cu eutectics is 150 to 200 HV, which shows a good accordance with the previous research.[30] The microhardness profiles further confirm that the transition zone widens further with the increasing pouring temperature. Interestingly, the hardness values of the eutectic region at 973 K (700 °C) seem to be mildly higher than these at 993 K (720 °C) for the VR 7.72 Cu/Al bimetals. The different eutectics layer spacings may be responsible for the hardness change. It should be noted that for Cu/Al bimetals fabricated at 993 K (720 °C), due to the solid solution strengthening of Ni, the microhardness values of Cu substrates near the interface are slightly higher than those fabricated at 973 K (700 °C).

IV. DISCUSSION

A. *The Reaction Mechanism of Ni Coating*

A deep understanding of the interfacial reaction behavior is of great significance. When the Cu insert contacts directly with the molten Al melt, an *in situ* oxide film can be formed during the mold-filling process by the radiation of heat from the molten Al before their contact.[20] The formed oxide film will act as a barrier that prevents the metallurgical bonding between the Cu insert and the Al melt. However, the Cu substrate has been coated by a 4 μm-thick Ni layer to inhibit surficial oxidation before casting in the present study. The Ni coating which serves as a sacrificial layer will be dissolved into the molten Al and promotes the metallurgical bonding between the Cu insert and the Al melt. It should be noted that the Ni coating will also be oxidized during the preheat treatment and compound casting process, and the formed Ni oxide film may hinder the interfacial metallurgical bonding.

Considering the as-received OM and SEM images of the Cu/Al bimetals, it is found that the interfacial reaction between the Ni coating and the molten Al during the casting process has a close relationship with the pouring temperature, more accurately, the thickness of the dissolved Cu substrate (d_{Cu}). When the pouring temperature is 953 K (680 °C), due to the short contact time and less energy absorbed for the solid–liquid interface, the Al melt solidifies rapidly, resulting in the local melting of the Ni coating, and some gaps and pores are easily detected. However, the Ni coating and part of the Cu matrix are detached off the surface and join in forming a continuous interface for Cu/Al bimetals fabricated at higher pouring temperature [973 K and 993 K (700 °C and 720 °C)]. It is thought that there exists a critical value (x, $112 < x < 191.3$ μm) for d_{Cu} to indicate the reaction of the Ni coating with the neighboring substrates. When d_{Cu} exceeds that critical value, the Ni content is so trace that no Ni-containing phase will be formed.

It has been discovered that particularly good suppression of Cu-Al IMCs may be obtained when the Cu/Al bimetal is formed from a Cu alloy containing about
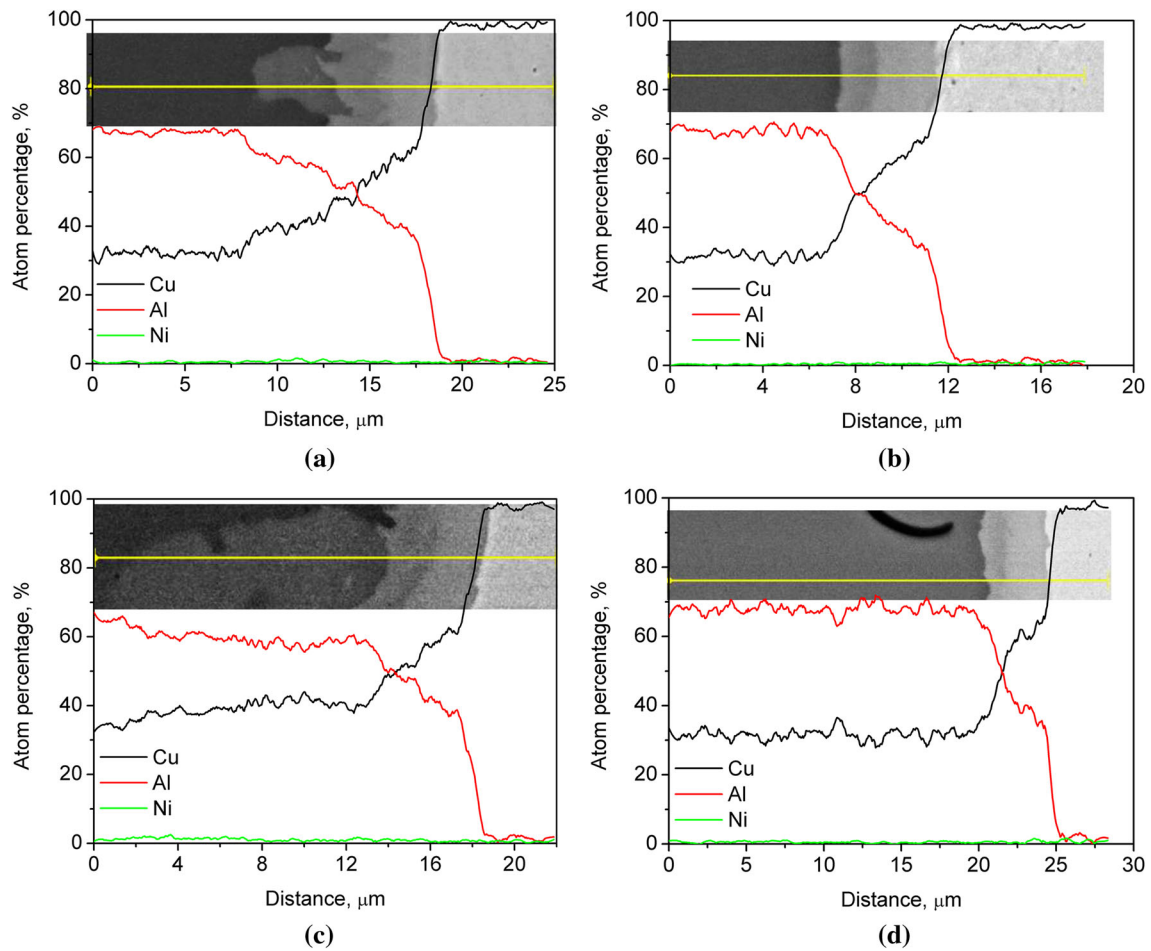
Fig. 10—EDS line scanning results of Cu/Al bimetals produced at different processing parameters: (*a*) 700 °C + VR 7.72; (*b*) 720 °C + VR 7.72; (*c*) 700 °C + VR 49.24; (*d*) 720 °C + VR 49.24.
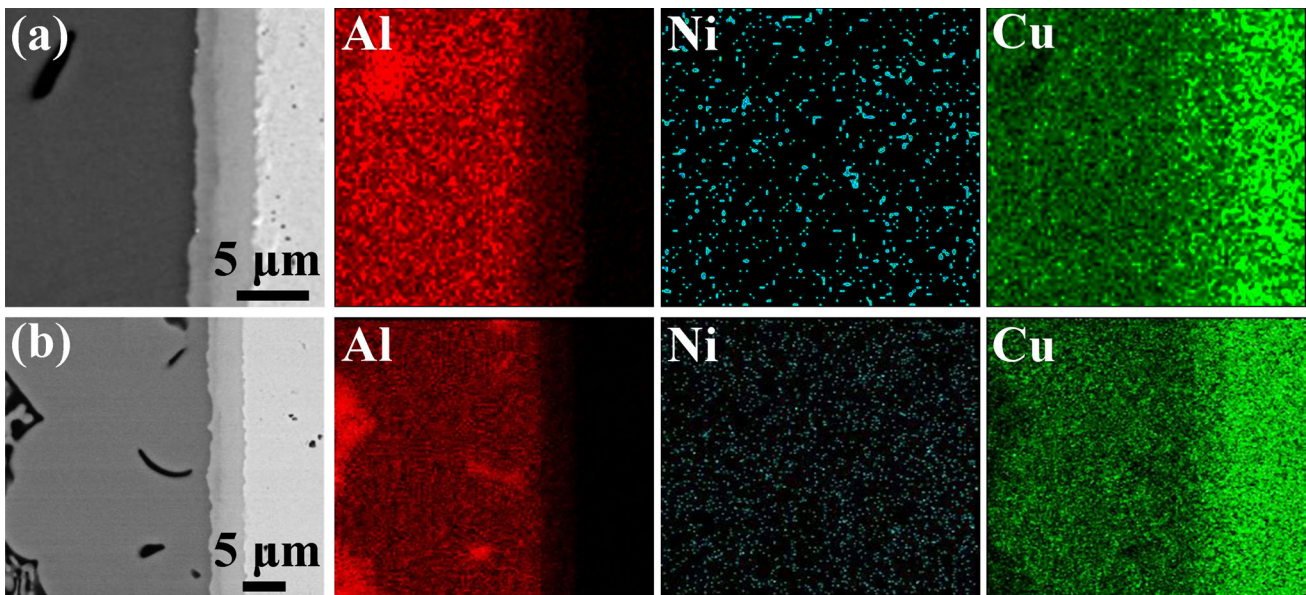

Fig. 11—Concentration mappings of Al, Ni, and Cu from Cu/Al bimetals produced at (*a*) 720 °C + VR 7.72 and (*b*) 720 °C + VR 49.24.
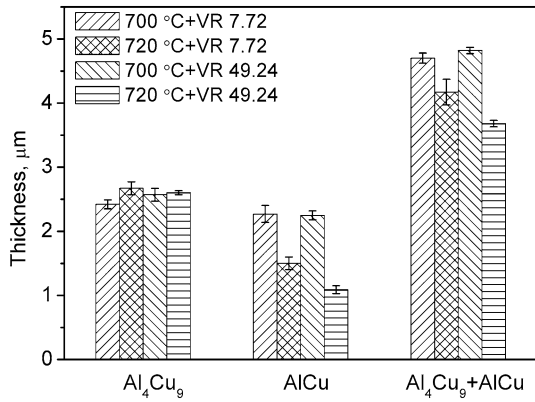
Fig. 12—The average thicknesses of Al_4Cu_9, AlCu, and Al_4Cu_9 + AlCu for Cu/Al bimetals produced at different processing parameters.
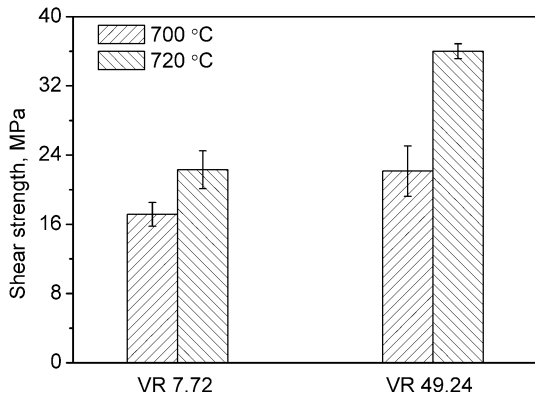

Fig. 13—Shear strengths of Cu/Al bimetals produced at different VRs and pouring temperatures.

15 ~ 30 pct Ni.[31] In the current study, the Ni coating together with the surface layer of the Cu matrix has been dissolved in the Al melt during the casting process, and the Ni content can be defined as

$$w_{Ni} = \frac{W_{Ni}}{W_{Tot}} = \frac{\rho_{Ni}sd_{Ni}}{\rho_{Ni}sd_{Ni} + \rho_{Cu}sd_{Cu}} = \frac{\rho_{Ni}d_{Ni}}{\rho_{Ni}d_{Ni} + \rho_{Cu}d_{Cu}},$$

[2]

where w_{Ni} is the weight percentage of Ni in the dissolved metal, W_{Ni} is the weight of the dissolved Ni coating, W_{Tot} is the sum weights of the dissolved Ni coating and Cu substrate; ρ and d are the density and thickness of the dissolved material indicated by the subscripts, respectively; and s is the contact area of solid–liquid bond. Due to the similar densities of Cu and Ni, Eq. [2] can be rewritten as:

$$w_{Ni} \approx \frac{d_{Ni}}{d_{Ni} + d_{Cu}}.$$

[3]

It is known that d_{Ni} is constant, 4 μm, and d_{Cu} can be obtained from Table I. The calculated results show that the weight percentages of Ni at the interface range from 2.1 to 3.5 pct. This calculated content of Ni is slightly higher than that measured by EDS. The reason could be attributed to the fact that the diffusion amount of Ni into the adhering Cu matrix and transition zone is neglected.

B. The Interfacial Microstructure of Cu/Al Bimetals

As seen in Figure 8, the microstructures at the transition zone vary at different VRs and pouring temperatures. The transition zone is comprised by two major layers with different thicknesses and morphologies. Layer I consists of the IMCs which are identified as Al_2Cu, AlCu (AlCuNi) and Al_4Cu_9. Layer II is mainly composed of the $[\alpha(Al) + Al_2Cu]_{eut}$ eutectics, and it can be divided into two sublayers: $[\alpha(Al) + Al_2Cu]_{eut} + Al_2Cu$; $[\alpha(Al) + Al_2Cu]_{eut}$ eutectics. The hypereutectic and eutectic microstructures are determined by the distribution of Cu atoms across the transition zone. The diffusion temperature and time are two key factors affecting the distribution of Cu atoms across the transition zone, as discussed in the previous research.[28]

The solidification time of $\alpha(Al)$ has a close relationship with the dissolution of the Cu substrate. The dissolution amount of the Cu substrate increases with the increasing solidification time of $\alpha(Al)$. Chen et al.[32] reported that the dissolved thickness of steel exhibits a linear relationship with the reaction time in the steel/aluminum system produced by hot dip method. However, in the current study, due to the non-isothermal dissolution of the Cu substrate, the thickness of the dissolved Cu shows a complicated relationship with the solidification time. It should be noted that the high-temperature interdiffusion between Cu and Al atoms to form solid solution at the interface will accelerate the local melting of the interface, resulting in an increased amount of Cu atoms to be dissolved.

On the other hand, by combining Figures 9 and 12, it is found that the growth of AlCuNi seems to promote the growth of AlCu, while it exerts no influence on the growth of Al_4Cu_9. The reaction process between the IMCs and Ni atoms is different from the previous study.[12] It has been reported that the activation energies of Al_2Cu, AlCu, and Al_4Cu_9 are found to be 127.5, 148.4 and 135.9 kJ/mol, respectively.[33] And the diffusivity of Cu in Al is greater than that of Al in Cu.[34] Therefore, Al_2Cu is thought to form first-and then the next reaction phase is Al_4Cu_9 and AlCu. Guo et al.[35] have verified the same results by using the effective heat of formation model. In this study, the AlCuNi phase grows between the Al_2Cu and AlCu phase when the pouring temperature is 973 K (700 °C). The underlying formation mechanism of AlCuNi needs to be further studied in future research.

C. The Interfacial Fracture Mechanism of Cu/Al Bimetals

In the current study, the Cu/Al bimetals with VR 49.24 have relatively higher shear strength than those with VR 7.72. According to the research of Durrant et al.[36] the Al matrix around the Cu insert will shrink during the solidification process, inducing a large
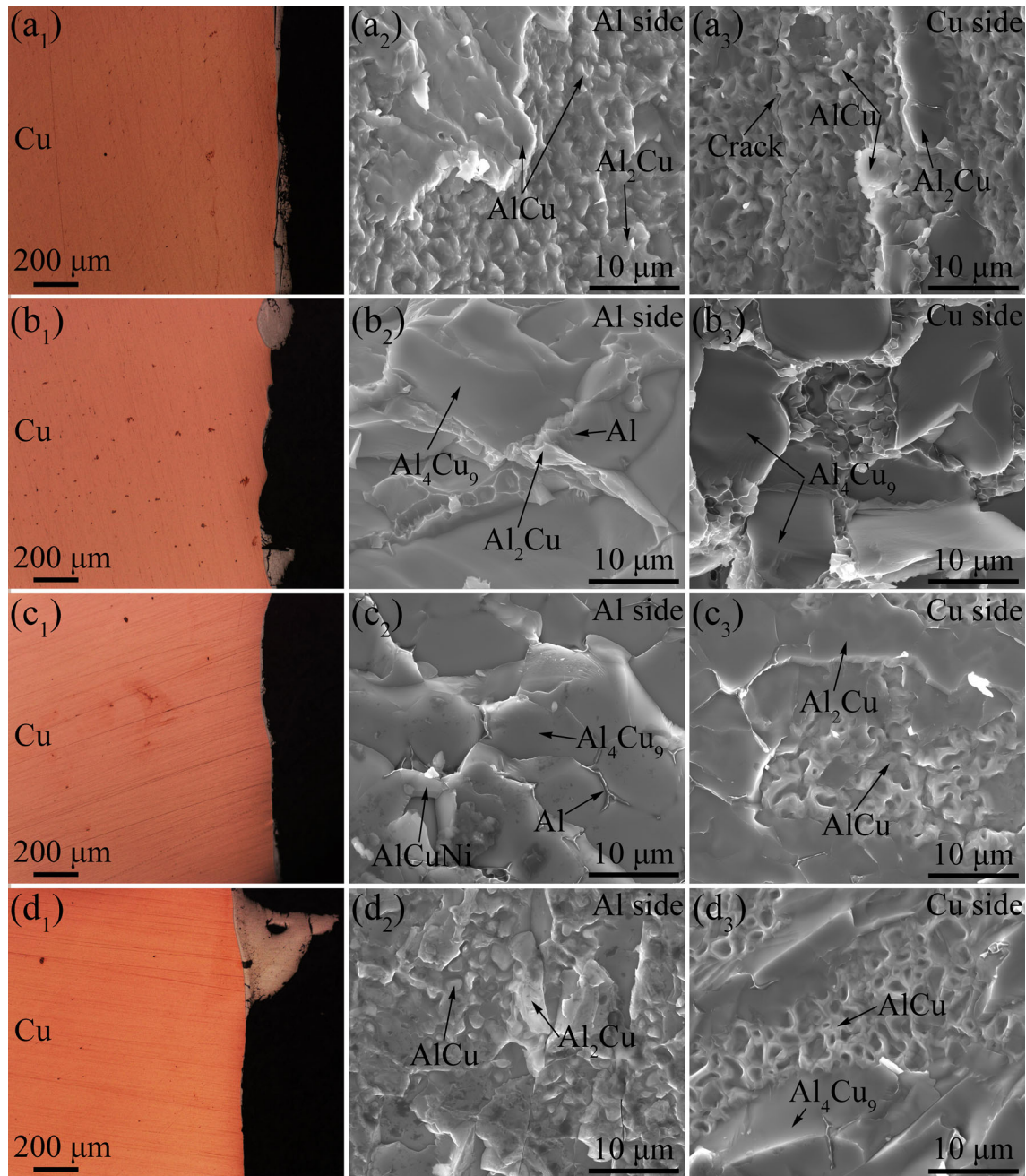
Fig. 14—Cross-section view and SEM micrographs of the shear fractured Cu/Al bimetals produced at different processing parameters: (a_1 through a_3) from 700 °C + VR 7.72 bimetal; (b_1 through b_3) from 720 °C + VR 7.72 bimetal; (c_1 through c_3) from 700 °C + VR 49.24 bimetal; (d_1 through d_3) from 720 °C + VR 49.24 bimetal.

compressive stress normal to the Cu substrate. Therefore, it is thought that the bimetallic samples with high VR have a higher bonding strength than those with low VR. Besides, as mentioned before, the Cu/Al samples with high VR mean that they have relatively low cooling rates. The lower the cooling rate, the more the interdiffusion between the substrates and precipitated phases. Thus, more and more IMCs have been dissolved in the transition zone. The thickness of the IMCs decreases with the increasing VR. It is known that the thickness of the IMCs is closely related to the interfacial bonding strength. Abbasi et al.[16] have reported that the

interfacial bonding strength of Cu/Al bimetals decreases with the increasing thickness of the IMCs. Therefore, the Cu/Al bimetals produced at 993 K + VR 49.24 (720 °C + VR 49.24) with the minimum thickness of AlCu + Al_4Cu_9 have the highest shear strength 36.01 MPa in this study.

It is widely accepted that the shear failure of Cu/Al bimetals mainly occurs on the hard brittle IMCs at the interface.[17,18] The reasons for this phenomenon are summarized in two aspects: (1) the high hardness and poor plasticity of the IMCs layer; (2) uncoordinated deformability among the IMCs, the α(Al) + Al_2Cu
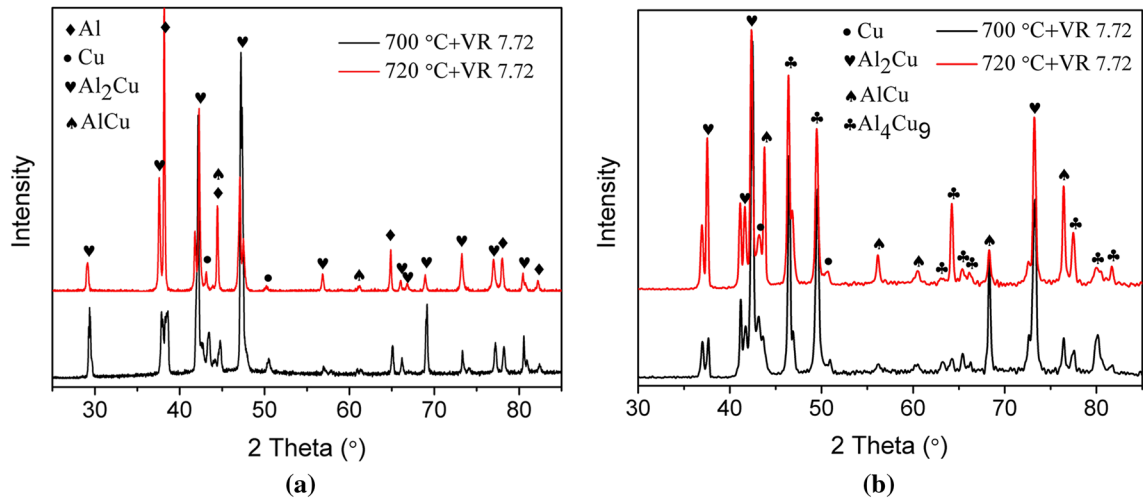
Fig. 15—XRD patterns on shear fractured Cu/Al bimetals fabricated at 700/720 °C + VR 7.72: (a) Al side; (b) Cu side.
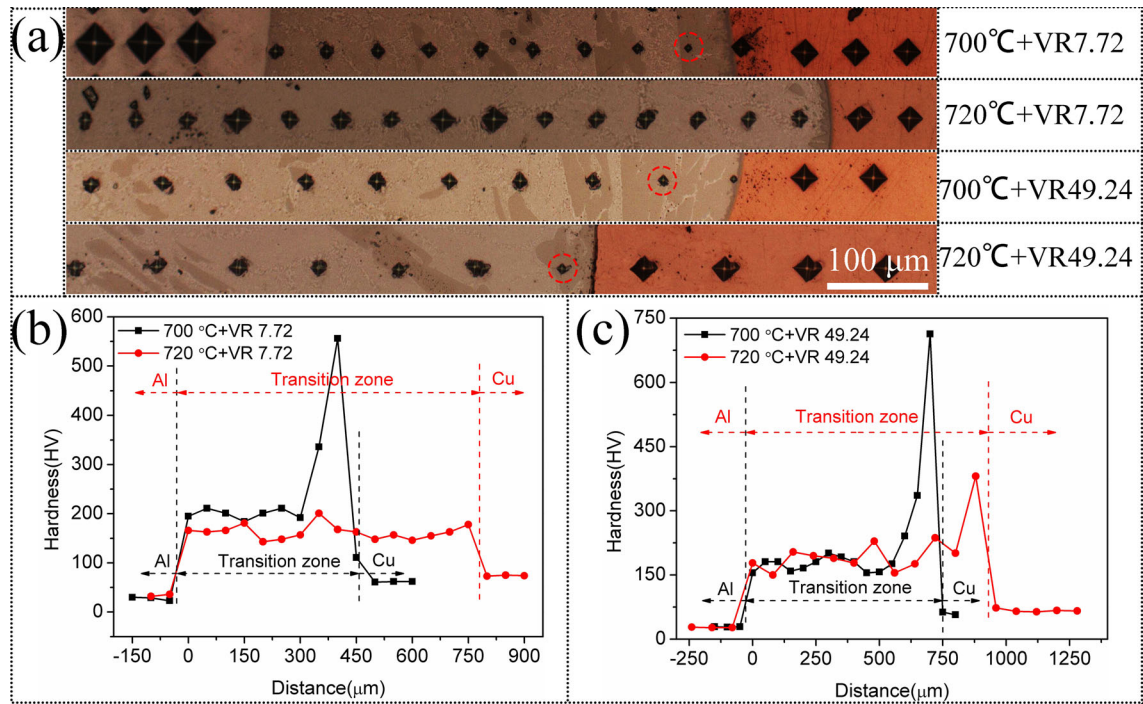

Fig. 16—OM image showing microhardness indentations of Cu/Al bimetals (a); microhardness evolution across the transition zone of Cu/Al bimetals: (b) VR 7.72, (c) VR 49.24.

eutectics, and Cu substrates. In the current study, layer II containing large amounts of α(Al) + Al$_2$Cu eutectics can be thought as a new component of the Al matrix. Thus, shear fracture is prone to occur at the hard brittle IMCs, *i.e.*, Al$_2$Cu, AlCu (AlCuNi) and Al$_4$Cu$_9$. As shown in Figure 14, Al$_2$Cu and AlCu are simultaneously visible on the surfaces of Cu and Al substrates after shear testing, and the crack may stretch to the adjacent eutectic layer. This result shows a good accordance with the previous studies in Cu/Al bimetals.[18,28]

V. CONCLUSIONS

This study investigates the effects of VRs and pouring temperatures on the interfacial microstructural evolution and mechanical properties of Ni-coated Cu/Al bimetals fabricated by compound casting. Conclusions can be drawn as follows:

(1) A short plateau of α(Al) solidification is captured at approximately 933 K (660 °C). With the increasing VR or pouring temperature, the solid-

ification time of α(Al) increases. A longer solid-ification time will induce a larger amount of the Cu atoms to be dissolved.

(2) At the pouring temperature of 953 K (680 °C), Ni coating is partly dissolved, and some micro-gaps exist at the interface. When the pouring temperature rises to higher values [973 K and 993 K (700 °C and 720 °C)], a continuous interface with α(Al) + Al_2Cu eutectics and IMCs is formed. The IMCs are identified as Al_2Cu, AlCu, and Al_4Cu_9.

(3) Ni coating participates while reacting with the IMCs when the pouring temperature is 973 K (700 °C), and a Ni-containing phase of AlCuNi is formed between the Al_2Cu and AlCu layers. When the pouring temperature increases to 993 K (720 °C), no Ni-containing phase precipitates.

(4) The Cu/Al bimetals produced at 993 K + VR 49.24 (720 °C + VR 49.24) have the highest shear strength of 36.01 MPa. Shear fracture mainly occurs at the hard brittle IMCs layer.

REFERENCES

1. D.J. Lloyd, M. Gallerneault, and R.B. Wagstaff: *Metall. Mater. Trans. A*, 2010, vol. 41A, pp. 2093–2103.
2. G. Liu, Q. Wang, T. Liu, B. Ye, H. Jiang, and W. Ding: *Mater. Sci. Eng. A*, 2017, vol. 696, pp. 208–15.
3. J. Park, H. Song, J.S. Kim, S.S. Sohn, and S. Lee: *Metall. Mater. Trans. A*, 2016, vol. 48A, pp. 57–62.
4. W. Jiang, G. Li, Z. Fan, L. Wang, and F. Liu: *Metall. Mater. Trans. A*, 2016, vol. 47A, pp. 2462–70.
5. W. Jiang, Z. Fan, G. Li, X. Liu, and F. Liu: *J. Alloy Compd.*, 2011, vol. 688, pp. 742–51.
6. H.G. Huang, P. Chen, and C. Ji: *Mater. Des.*, 2017, vol. 118, pp. 233–44.
7. R. Kocich, L. Kunčická, A. Macháčková, and M. Šofer: *Mater. Des.*, 2017, vol. 123, pp. 137–46.
8. K. Oh-ishi, K. Edalati, H.S. Kim, K. Hono, and Z. Horita: *Acta Mater.*, 2013, vol. 61, pp. 3482–89.
9. H. Amani and M. Soltanieh: *Metall. Mater. Trans. B*, 2016, vol. 47B, pp. 2524–34.
10. W. Zhang, Y. Shen, Y. Yan, and R. Guo: *Mater. Sci. Eng. A*, 2017, vol. 690, pp. 355–64.
11. Q. Wang, M.A. Osborne, E.C. Tuohy: *Methods of Manufacturing Induction Rotors with Conductor Bars Having High Conductivity*, 2014, US 8701270 B2.
12. Y. Hu, Y. Chen, L. Li, H. Hu, and Z. Zhu: *Trans. Nonferr. Met. Soc. China*, 2016, vol. 26, pp. 1555–63.
13. J.L. Murray: *Int. Met. Rev.*, 1985, vol. 30, pp. 211–34.
14. L.Y. Sheng, F. Yang, T.F. Xi, C. Lai, and H.Q. Ye: *Composites B*, 2011, vol. 42, pp. 1468–73.
15. W.B. Lee, K.S. Bang, and S.B. Jung: *J. Alloy Compd.*, 2005, vol. 390, pp. 212–19.
16. M. Abbasi, A.K. Taheri, and M.T. Salehi: *J. Alloy Compd.*, 2001, vol. 319, pp. 233–41.
17. Y. Su, X. Liu, H. Huang, X. Liu, and J. Xie: *Metall. Mater. Trans. A*, 2011, vol. 42, pp. 4088–99.
18. T. Liu, Q. Wang, Y. Sui, Q. Wang, and W. Ding: *Mater. Des.*, 2016, vol. 89, pp. 1137–46.
19. J. Zhao, J. Jie, F. Chen, H. Chen, T. Li, and Z. Cao: *Trans. Nonferr. Met. Soc. China*, 2014, vol. 24, pp. 1659–65.
20. Q. Han: *Metall. Mater. Trans. B*, 2016, vol. 47B, pp. 3266–73.
21. M. Sun, S.T. Niknejad, G. Zhang, M.K. Lee, L. Wu, and Y. Zhou: *Mater. Des.*, 2015, vol. 87, pp. 905–13.
22. H. Wang, L. Liu, and F. Liu: *Mater. Des.*, 2013, vol. 50, pp. 463–66.
23. H. Okamoto: *J. Phase Equilib.*, 1993, vol. 14, pp. 257–59.
24. R.D. Doherty and E.A. Feest: *J. Jpn. Inst. Met.*, 1971, vol. 99, pp. 102–103.
25. A. Shabani, M.R. Toroghinejad, and A. Shafyei: *Mater. Des.*, 2012, vol. 40, pp. 212–20.
26. M. Pintore, T. Mittler, W. Volk, O. Starykov, and B. Tonn: *Int. J. Met.*, 2017, vol. 12, pp. 1–10.
27. R. Chen, Y. Shi, Q. Xu, and B. Liu: *Trans. Nonferr. Met. Soc. China*, 2014, vol. 24, pp. 1645–52.
28. G. Liu, Q. Wang, L. Zhang, B. Ye, H. Jiang, and W. Ding: *Metall. Mater. Trans. A*, 2018, vol. 49A, pp. 661–72.
29. L.Y. Sheng, F. Yang, T.F. Xi, J.T. Guo, and H.Q. Ye: *Mater. Sci. Eng. A*, 2012, vol. 555, pp. 131–38.
30. Y. Zhang, T. Yamane, K. Hirao, and Y. Minamino: *J. Mater. Sci.*, 1991, vol. 26, pp. 5799–5805.
31. J.F. Breedis and J.C. Fister: *Copper Alloys for Suppressing Growth of Cu-Al Intermetallic Compounds*, 1985, US 4498121.
32. S. Chen, D. Yang, M. Zhang, H. Huang, and X. Zhao: *Metall. Mater. Trans. A*, 2016, vol. 47A, pp. 5088–5100.
33. Y. Funamizu and K. Watanabe: *Trans. Jpn. Inst. Met.*, 1971, vol. 12, pp. 147–52.
34. C.Y. Chen and W.S. Hwang: *Mater. Trans.*, 2007, vol. 48, pp. 1938–47.
35. Y. Guo, G. Liu, H. Jin, Z. Shi, and G. Qiao: *J. Mater. Sci.*, 2010, vol. 46, pp. 2467–73.
36. G. Durrant, M. Gallerneault, and B. Cantor: *J. Mater. Sci.*, 1995, vol. 31, pp. 589–602.